

The Galactic Center Molecular Tornado Driven by Magnetic Squeezing Mechanism

Yoshiaki SOFUE

*Institute of Astronomy, The University of Tokyo, Mitaka, Tokyo 181-0015
sofue@ioa.s.u-tokyo.ac.jp*

(Received 2006 August 29; accepted 2006 November 6)

Abstract

Based on an analysis of the CO line-survey data, we report on peculiar properties of a helical-spur object of molecular gas at a radial velocity of $V_{\text{lsr}} \sim 70 \text{ km s}^{-1}$ extending vertically from the galactic plane at $l = 1^\circ 2'$ to high latitudes of $b \sim \pm 0^\circ 6'$. We call the object the Galactic Center molecular Tornado (GCT). The tornado is 170 pc ($1^\circ 2'$) long and 14 pc ($6'$) wide, and is spinning at a rotation velocity of $\sim 30 \text{ km s}^{-1}$ in the same sense as, but with much steeper velocity gradient than, the galactic rotation. The coherent collimation and helical structure suggest that the tornado is related to an ordered vertical magnetic field. We propose a magnetic squeezing mechanism such that a vertical magnetic tube or a root of a large-scale prominence-like magnetic flux is twisted and squeezed by a molecular cloud in galactic rotation, and the gas is pushed out along the magnetic tube. The angular momentum of the cloud is lost along the twisting magnetic tube, which promotes gravitational collapse of the cloud and enhances star formation.

Key words: Galaxy: center — Galaxy; jet — ISM: molecular cloud — ISM: magnetic field

1. Introduction

Morris et al. (2006) recently reported a double-helix nebula above the Galactic Center by $24 \mu\text{m}$ imaging with the Spitzer Space Telescope. The nebula shows coherent helical strands of warm dust vertically extending toward high positive latitudes. They interpret the helix as being due to a torsional Alfvén wave in a twisted vertical magnetic field driven by the circum nuclear rotating disk. Another type of large helical jet of neutral gas was noticed in the G40–15 ($l \sim 45^\circ$, $b \sim -15^\circ$) region in the HI survey data (Hartmann & Burton 1997) at a radial velocity of about 90 km s^{-1} , which extends from the G30+00 star-forming region toward negative high latitudes with a length of more than 2 kpc (Sofue et al. 2004). This HI jet is interpreted as being due to a large-scale twisting magnetic acceleration of interstellar gas driven by gravitational contraction of a rotating giant molecular cloud in the 4-kpc molecular ring associated with the W43 star-forming complex.

Oka et al. (1998) performed a large-scale CO line survey of the Galactic Center using the Nobeyama 45-m telescope. They noticed a large molecular complex at $l = 1^\circ 1' - 1^\circ 6'$ and $b = -0^\circ 3' \sim +0^\circ 5'$ at $V_{\text{lsr}} = 30$ to 140 km s^{-1} , which they call a molecular flare. The flare region contains a number of shells and filaments with various velocity anomalies (Oka et al. 2001).

In this paper, we analyze Oka et al.’s CO data in the G1.2+0.0 region, and report on a prominent spur of molecular gas extending to high latitudes, which we call the Galactic Center molecular Tornado (GCT). We interpret the tornado as being a new type of vertical magnetized structure of molecular gas, and propose a magnetic twist-squeezing model for its origin. We use the word tornado instead of jet, because the object is rapidly rotating around its axis and its vertical velocity is not large enough compared with the rotation. Moreover, the gas may appear to be in quasi-hydrostatic equilibrium in the

vertical direction along a magnetic tube, and hence it is not dynamic as a jet.

2. Data and Analysis

2.1. Intensity Maps

We used the $^{12}\text{C}^{16}\text{O}(J = 1 - 0)$ -line survey of the Galactic Center obtained at 115 GHz by the 45-m telescope at the Nobeyama Radio Observatory by Oka et al. (1998). The beam width of the telescope was $15''$ and grid spacing was $34''$, and the final maps were smoothed to a resolution of $1'$. The survey covered a region at $358^\circ < l < 3^\circ$, $-40' < b < +36'$ and $-220 < V_{\text{lsr}} < +220 \text{ km s}^{-1}$, and the data consist of 88 velocity-channeled cube in (l, b, V) space with a velocity channel interval of 5 km s^{-1} .

In channel maps of Oka et al. (1998), we noticed a prominent spur-like feature at $l \sim 1^\circ 2'$ within the molecular flare region. In figure 1, we reproduce from their data a CO intensity integrated over $V_{\text{lsr}} = 25$ to 85 km s^{-1} for a region around the molecular flare region at $(l, b) \sim (1^\circ 2', 0^\circ)$ (G1.2+0.0). The map shows a prominent spur extending toward positive latitudes almost perpendicularly to the galactic plane, reaching to G1.2+0.5. A counterpart to this spur is found at G1.25–0.4 extending toward negative latitude almost symmetrically to the northern spur with respect to the galactic plane. We call this feature the Galactic Center Tornado (GCT). Figure 2 enlarges the major part of the northern tornado.

2.2. Molecular Tornado

Figure 3 is the same as figure 1, but with color-coded intensities, where the blue (B), green (G) and red (R) colored brightness indicate the integrated CO intensities in 5 km s^{-1} velocity intervals at 45, 70, and 95 km s^{-1} , respectively. Lines A–A', B–B' and C–C' indicate the positions along which we made longitude-velocity diagrams (discussed later; see figure

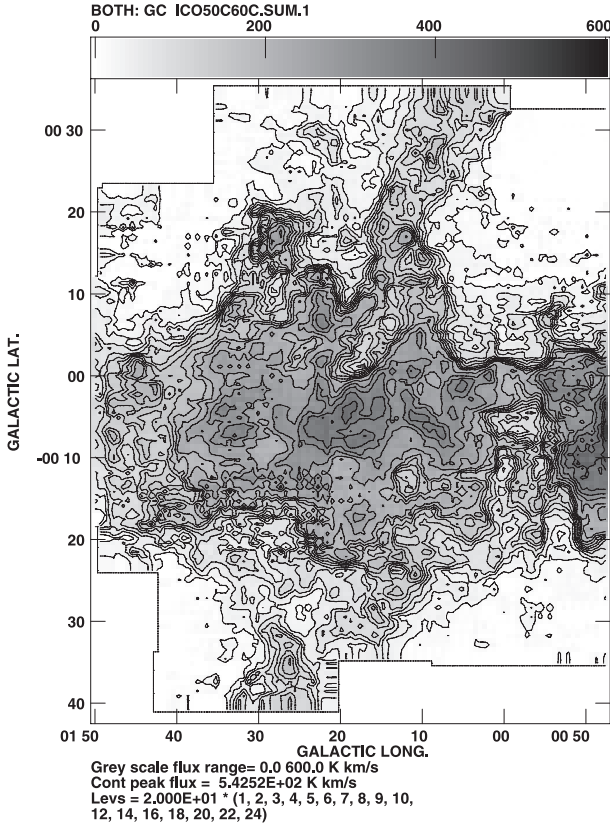


Fig. 1. CO intensity of the Galactic Center Tornado (GCT), as integrated from 25 to 85 km s⁻¹.

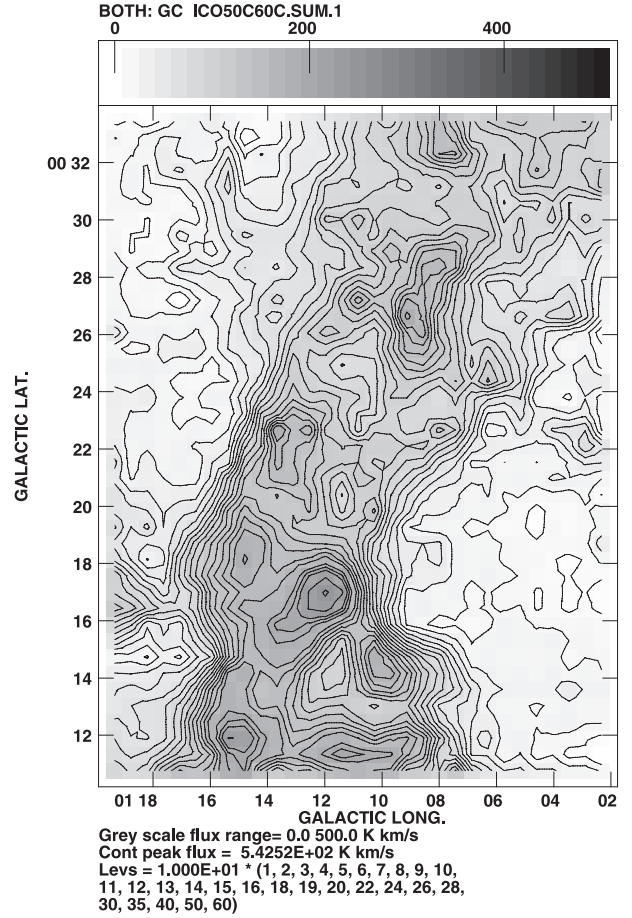


Fig. 2. Close up of the northern part of the Galactic Center Tornado.

5). Figure 4 shows the velocity field of the GCT, which was obtained by a moment-1 map in the velocity range from 25 to 100 km s⁻¹.

The northern tornado reaches to $b \sim 33'$, and the southern one to $\sim -40'$. The whole length from the top to bottom is approximately $1^{\circ}22'$. Since the radial velocities reach almost 100 km s⁻¹, the feature is without doubt located associated with the Galactic Center. If we take a GC distance of 8 kpc, the vertical extent is as long as 170 pc, and the projected distance from GC is 170 pc. It is not straight, but waves at a wavelength of $\sim 15'$ (40 pc). The intensity channel map at ~ 58 km s⁻¹ (figure 1) indicates that the spur comprises a helix of filamentary molecular gas. The width of the tornado is about $6'$ (14 pc) with a plateau or double horn-like cross section, and both side edges are clearly cut, suggesting a cylindrical structure.

The morphology of the GCT, particularly the northern tornado, is very similar to that reported for the double-helix nebula (Morris et al. 2006). The tornado is composed of two strands of helices, as is indeed observed in double-helix nebula.

2.3. Molecular Mass and Density

The total mass of the GCT depends on the region to be integrated. Here, we estimate the mass included in the region shown in figure 3. The mean CO intensity within this area is $I_{\text{CO}} = 73.4$ K km s⁻¹ in T_A . Taking a main-beam efficiency of 0.52 (Oka et al. 1998), we obtain a mean CO intensity of 141 K km s⁻¹. We assume a conversion factor of 0.3-times that

in the solar neighborhood, or

$$X = 0.3X_{\odot}$$

with

$$X_{\odot} = 2.0 \times 10^{20} \text{ H}_2 \text{ cm}^{-2} [\text{K km s}^{-1}]^{-1}$$

for the Milky Way (Arimoto et al. 1996).

Then, we obtain a column density of molecular hydrogen of

$$N_{\text{H}_2} = 8.5 \times 10^{21} \text{ H}_2 \text{ cm}^{-2}$$

averaged in an area of $18 \times 24'$. By multiplying the whole area of figure 3 and the mass per molecular hydrogen including metals (1/0.73), we obtain the total mass of gas within the squared area of figure 3 to be

$$M = 4.3 \times 10^5 M_{\odot}.$$

For the observed width of $6'$ of the GCT instead of $18'$ for the area in figure 3, we have a column density that is three-times this value, or

$$N_{\text{H}_2} \sim 2.5 \times 10^{22} \text{ H}_2 \text{ cm}^{-2},$$

corresponding to a column mass density of 0.12 g cm^{-2} . This yields a space density of

$$n_{\text{H}_2} = 5.9 \times 10^2 \text{ H}_2 \text{ cm}^{-3}$$

or

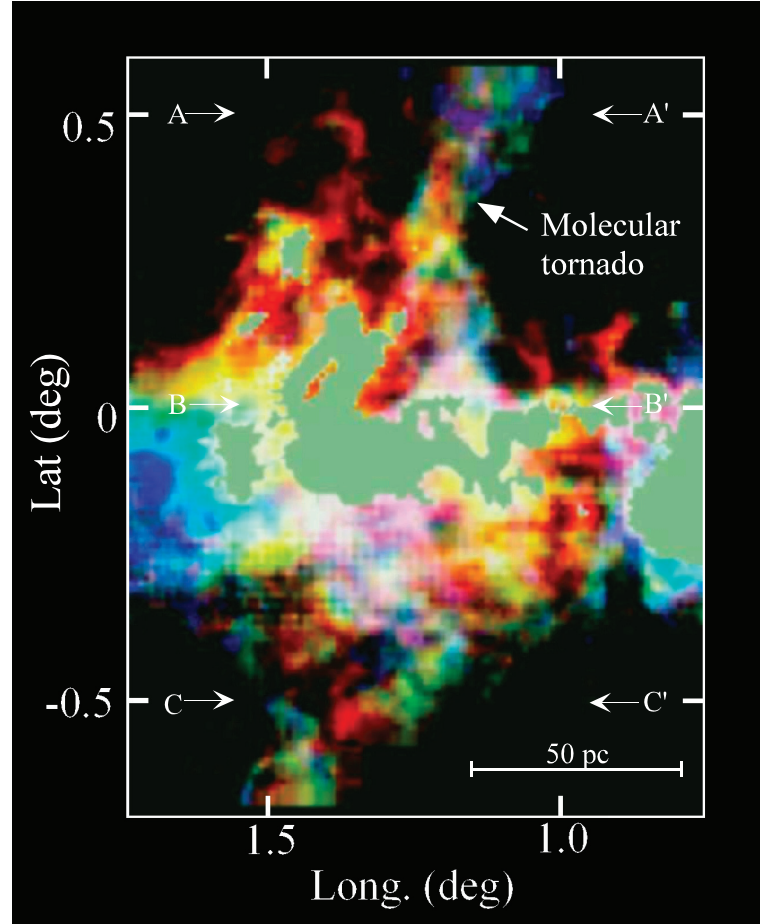


Fig. 3. Composite CO intensity distribution of the Galactic Center Tornado. The red, green and blue (RGB) colored brightnesses represent integrated intensities over 5 km s^{-1} around radial velocities of 45, 60, and 75 km s^{-1} , respectively. Horizontal lines indicate the positions across which we made longitude-velocity diagrams, as shown in figure 5.

$$\rho \sim 2.7 \times 10^{-21} \text{ g cm}^{-3}.$$

Although the tornado feature is contaminated by the disk component near the galactic plane, we may estimate that about three-times the thus-estimated mass is included in the whole feature from the northern top to the southern end. Namely, we estimate

$$M \sim 1.2 \times 10^6 M_{\odot}$$

for the entire GCT feature appearing in figure 1.

2.4. Rotation and Kinematics

In order to measure the rotation velocity more quantitatively, we made longitude-velocity (LV) diagrams across the GCT at $b = 0.5, 0$ and -0.5 (figure 5). The wide-area LV diagrams (upper panels) show that the GCT have much steeper gradients compared to the surrounding galactic center gas. The high-velocity spin motion of GCT is in the same sense as the galactic rotation with its highest rotation in the mid-plane. The mid-plane LV ridge appears to be in touch with the high-velocity feature at G1.27+0.0 with $V_{\text{lsr}} > 100 \text{ km s}^{-1}$, which Oka et al. (2001) interpreted as being due to a hyper-energetic expanding CO shell.

From the LV diagrams, we can estimate the velocity gradients at $b \sim \pm 0.5$ to be $\sim 60 \text{ km s}^{-1}$ across a diameter of $6'$, or

$$dv/dl \sim 600 \text{ km s}^{-1} \text{ deg}^{-1} \sim 4000 \text{ km s}^{-1} \text{ kpc}^{-1}.$$

Namely, the GCT is spinning at 30 km s^{-1} at the side edges (surface) in the same sense as the galactic rotation. Interestingly, the LV diagram near to the galactic plane shows a very high-speed spin, as high as $\pm 50 \text{ km s}^{-1}$ within $\sim 9'$ (21 pc), or $V_{\text{lsr}} = 0$ to $\sim 100 \text{ km s}^{-1}$ from $l = 1.1$ to 1.25 . The velocity gradient is, therefore,

$$dv/dl = 670 \text{ km s}^{-1} \text{ deg}^{-1} \sim 4800 \text{ km s}^{-1} \text{ kpc}^{-1}.$$

These velocity gradients are much steeper than that for usual galactic rotation, and are almost comparable to that of the circum-nuclear disk. Sofue (2006) has developed a method to determine the distances to arms in the GC direction using a velocity gradient, dv/dl , by which the galacto-centric distance of an LV ridge is calculated by

$$R \simeq 28(V_{\text{rot}}/200 \text{ km s}^{-1})/(dv/dl^{\circ}) \text{ [kpc]}$$

(Sofue 2006), where $V_{\text{rot}} = 200 \text{ km s}^{-1}$ is the rotation velocity and dv/dl° is the velocity gradient measured in $\text{km s}^{-1} \text{ deg}^{-1}$.

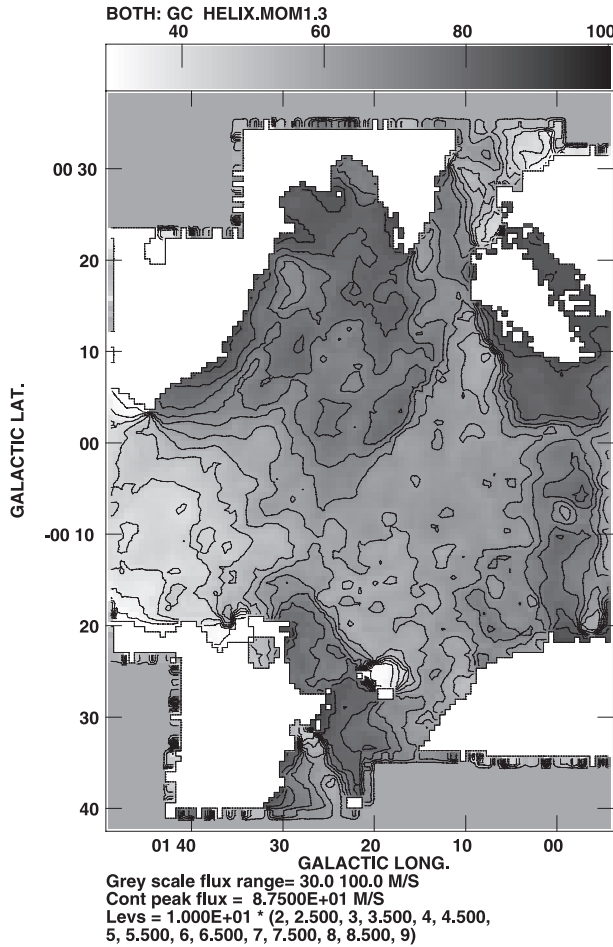


Fig. 4. Velocity field (moment 1 map) of CO gas in the tornado region around G1.2+0.0. Note steeper velocity gradients in the GCT compared to that near the galactic plane.

Applying this method to the above velocity gradients, we obtain galacto-centric distances of 47 and 42 pc, respectively, for the tornado and the mid-plane high-rotation region. These distances are clearly inconsistent with the projected distance of 170 pc for our features. We may thus attribute the observed velocity gradients to local rotation, or spin motion.

We here emphasize that the sense of the spin of GCT both at positive and negative latitudes as well as that in the mid plane is the same. Moreover, the mid-plane rotation is extremely high, as much as 50 km s^{-1} . Such acceleration of the spin motion may be due to vortex concentration induced by evacuation of gas from the mid-plane along the magnetic tube.

It is interesting to note that the high-rotation mid-plane gas is positionally close to the hyper-energetic double shells CO 1.27+0.01 found by Oka et al. (1998, 2001) at $V_{\text{lsr}} = 100$ to 200 km s^{-1} , which has a velocity width as large as $\sim 100 \text{ km s}^{-1}$ and a size of $\sim 10 \text{ pc}$.

2.5. Identification with Other Wavelength Data

The molecular gas complex around G1.2+00 is apparently associated with two radio sources. One source is a compact radio source, G1.332+0.106, which has a peak flux at 10 GHz of 0.76 Jy per beam, total flux of 1.38 Jy, and the angular size

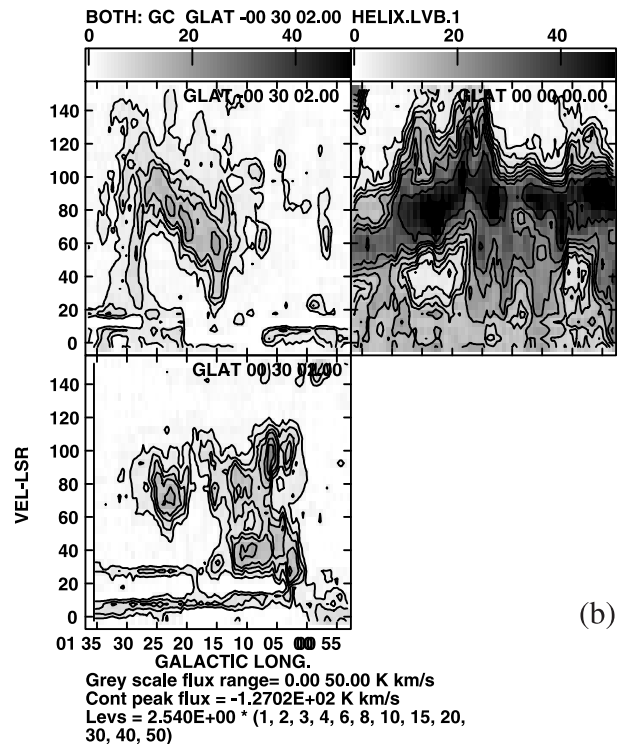
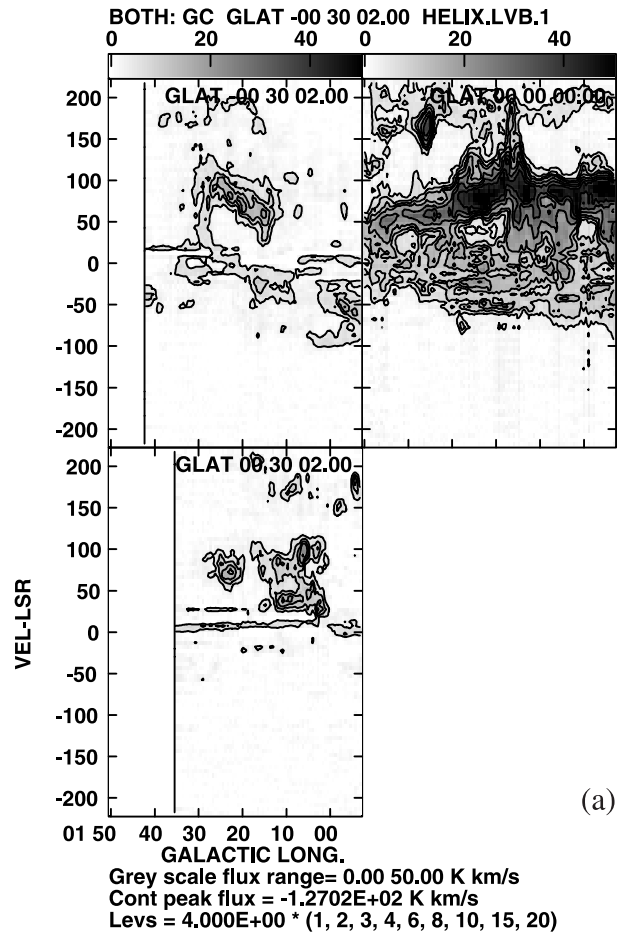


Fig. 5. (a) LV diagrams across the GCT along line A-A' in figure 3 at $b = +0^\circ.5$ (bottom panel), along B-B' at $b = 0^\circ$ (top right), and C-C' at $-0^\circ.5$ (top left). (b) The same as figure (a), but enlarged for the GCT part.

is 4.0 arc mins, according to the 10 GHz survey by Handa et al. (1987). This source positionally coincides with the high-velocity compact expanding shell CO 1.27+0.01 of Oka et al. (1998, 2001). A faint stellar cluster appears to be associated, as shown in the MSX image (Price et al. 2001). Another source is a prominent HII region. Sgr D at G1.13–0.05 (LaRosa et al. 2000), identified by a bright extended far-infrared nebula in the MSX 26 μm map (Price et al. 2001). However, this source is positionally remote from the expanding molecular shell and shocks, and may not be related to the present GCT structure.

We have tried to identify the GCT with some spur-like features in maps and images at different wavelengths. Radio continuum maps at 10 GHz (Handa et al. 1987) and 2.7 GHz (Reich et al. 1990) show wide spurs extending toward the north from the G1.2+00 region, but its correlation with the CO tornado is not clear. We also recognize a faint spur of warm dust in mid-infrared images at 26 μm by MSX (Price et al. 2001) and a spur of a dark cloud in a near-IR image from 2MASS (Strutskie et al. 2006). Quantitative analyses of the infrared data are, however, a subject for future work.

3. Twist-Squeezing Magnetic Model for the GCT

3.1. Energetics

In order to discuss possible mechanisms to produce the GCT, we estimate some energies using the observed quantities. Table 1 summarizes the estimated results.

The mass of the tornado is $M \sim 1.2 \times 10^6 M_\odot$. The gravitational energy required to lift this mass from the galactic plane to its height of $\sim 20'$, or $h \sim 50$ pc, is given by

$$E_{\text{grav}} = Mgh$$

with g being the vertical acceleration. The vertical acceleration, g , is estimated from the thickness of the molecular ring around the Galactic Center, which was measured to be $h_0 \sim 10$ pc, (e.g. Sofue 1995). Since the velocity dispersion of molecular gas is on the order of $\sigma \sim 10$ km s $^{-1}$, we find

$$g \sim \sigma^2 / h_0 \sim 10 \text{ (km s}^{-1}\text{)}^2 / \text{pc.}$$

Then, the gravitational energy is calculated as

$$E_{\text{grav}} \sim 1.2 \times 10^6 M_\odot gh \sim 1.3 \times 10^{52} \text{ ergs.}$$

The GCT is spinning at a surface speed of about $v \sim 30$ km s $^{-1}$ on the average, except for the high-velocity clump near the galactic plane. This yields a rotational kinetic energy on the order of

$$E_{\text{spin}} \sim (1/2)Mv^2 \sim 1.2 \times 10^{52} \text{ ergs,}$$

about the same as the gravitational energy.

3.2. Kinematics

Rotation of the GCT around its axis causes a centrifugal force of

$$f_c = v^2 / r$$

for the feature to spread out, where v and r are the rotation velocity and radius, respectively. In order to maintain the coherent tornado structure, some force to confine the gas close to its axis is needed. Gravitational force could be one possibility. The self-gravitation by the cloud on the tornado surface is given by

$$f_g \sim \pi G \rho r,$$

where G and ρ are the gravitational constant and the gas density, respectively. If

$$\eta = f_g / f_c$$

is greater than unity, the tornado is gravitationally bound, while otherwise it is unbound. By inserting the observed values (table 1), we obtain

$$\eta = \pi G m_{\text{H}} N r v^{-2} \sim 0.01.$$

We thus conclude that the tornado structure is not gravitationally bound by the cloud mass, as is naturally supposed from its morphology.

3.3. Field Strength Required for Magnetic Confinement

In order to maintain the coherent structure of the tornado, some external pressure or force is required to confine the gas in a cylinder. The most plausible mechanism is magnetic confinement, as suggested by the collimated helical structure. An aligned external magnetic field can act to confine the interstellar gas to a thin tube by its magnetic tension, which is on the order of

$$f_m \sim dp_{\text{mag}} / dr,$$

where $p_{\text{mag}} = B^2 / 8\pi$ is the magnetic pressure. In order for the centrifugal force to be balanced by the magnetic tension, we need

$$f_c \sim f_m,$$

or

$$dp_m / dr \sim \rho v^2 / r.$$

Then, we obtain

$$B \sim (4\pi\rho v^2)^{1/2}.$$

For $\rho \sim 5.9 \times 10^2$ H $_2$ cm $^{-3}$ or $\rho \sim 2.7 \times 10^{-21}$ g cm $^{-3}$, we have $B \sim 0.4$ mG. The corresponding Alfvén velocity is obviously comparable to the rotational velocity, $V_A \sim B / \sqrt{4\pi\rho} \sim 30$ km s $^{-1}$.

Here, we introduce the dynamic β value, defined by the ratio of kinetic to the required magnetic energy densities, as

$$\beta_d = (1/2\rho v^2) / (B^2 / 8\pi).$$

For the above values, we have $\beta_d \sim 1$. If the dynamic β is greater than unity, a gas cloud will expand due to its centrifugal force, and the gas can be confined in a magnetic tube, if $\beta_d < 1$.

It has been suggested that the galactic center is filled by a strong vertical magnetic field on the order of mG (Morris & Yuzef-Zadeh 1985; Tsuboi et al. 1986; Sofue et al. 1987). If such a field penetrates a molecular gas in the G1.2+0.0 region, the dynamic β would be as small as $\beta_d \sim 0.2$, and the gas would be passive to the magnetic field, being confined in a tube. The maximum magnetic field strength allowed in the galactic center disk is calculated by balancing the magnetic energy with the kinetic energy density of the galactic with $V_{\text{gal,rot}} = 200$ km s $^{-1}$, which corresponds to a magnetic strength of $B_{\text{max:gal}} \sim 4$ mG.

These estimates stimulate us to suggest a mechanism by which a gas cloud in galactic rotation is confined in a thin, but strong, magnetic tube. We now suggest a scenario to produce a vertical magnetic tornado.

Table 1. Parameters and energetics of the Galactic Center Tornado

Molecular column density [†] ‡	$N_{\text{H}_2} \sim 2.5 \times 10^{22} \text{ H}_2 \text{ cm}^{-2}$
Molecular density for 14 pc depth	$n_{\text{H}_2} \sim 5.9 \times 10^2 \text{ H}_2 \text{ cm}^{-3}$
	$\rho \sim 2.7 \times 10^{-21} \text{ g cm}^{-3}$
Total molecular gas mass [†]	$M \sim 1.2 \times 10^6 M_\odot$
Kinetic energy by galactic rotation	$E_{\text{gal.rot}} \sim 5 \times 10^{53} \text{ ergs}$
Kinetic energy by spin	$E_{\text{spin}} \sim 1.2 \times 10^{52} \text{ ergs}$
Gravitational energy	$E_{\text{grav}} \sim 1.3 \times 10^{52} \text{ ergs}$
Kinetic energy density for galactic rotation	$u_{\text{gal.rot}} \sim 5 \times 10^{-7} \text{ ergs cm}^{-3}$
Kinetic energy density for spin	$u_{\text{spin}} \sim 1.2 \times 10^{-8} \text{ ergs cm}^{-3}$
Gravitational energy density	$u_{\text{grav}} \sim 1.4 \times 10^{-8} \text{ ergs cm}^{-3}$
Magnetic energy density to confine gas	$u_{\text{mag}} \sim u_{\text{spin}} \sim 1.4 \times 10^{-8} \text{ ergs cm}^{-3}$
Magnetic field strength	$B \sim 0.4 \text{ mG}$
Max. magnetic energy density equiv. to gal. rot.	$u_{\text{mag,max}} \sim u_{\text{gal.rot}} \sim 5 \times 10^{-7} \text{ ergs cm}^{-3}$
Max. magnetic strength allowed in galactic rotation	$B_{\text{max}} \sim 3.7 \text{ mG}$

† Conversion factor of $X = 0.3X_\odot$ with $X_\odot = 2.0 \times 10^{20} \text{ H}_2 \text{ cm}^{-2} (\text{K km s}^{-1})^{-1}$; total to hydrogen mass ratio 1/0.73; galactic center distance 8 kpc.

‡ Representative values at $b \sim +0^\circ$.

3.4. Magnetic Twist-Squeezing Mechanism

Suppose that a gas cloud is orbiting around the Galactic Center while obeying the galactic rotation, and that the cloud is penetrated by a large-scale vertical magnetic field anchored to the halo at rest. If the dynamic β is larger than unity, or the galactic rotation energy exceeds that of the magnetic field, the orbiting rotation and spin of the cloud twist the magnetic field. The magnetic tube is twisted and squeezed while becoming thinner (figure 6). This process is the same as that proposed for the double-helix nebula by Morris et al. (2006) as the torsional Alfvén wave excited by rapid rotation of the circum-nuclear disk.

A twisting amplification of the magnetic field will continue until the dynamic $\beta_{\text{d:gal}}$ by galactic rotation becomes unity, or until B reaches the maximum value of $B_{\text{max:gal}} \sim 4 \text{ mG}$. The growth time of the field twist, namely the time for one turn of twist, is on the order of the period of the epicyclic rotation of the cloud, which is on the order of the galactic rotation period, or

$$t \sim 2\pi/\Omega \sim 2\pi R V_{\text{rot}} \sim 5 \text{ Myr},$$

where $R = 170 \text{ pc}$ is the galacto-centric distance of the cloud.

However, before reaching the maximum, as the magnetic strength is amplified, the local β value due to the gas pressure and the internal motion will decrease and become less than unity. Then, the magnetic tension within the tube exceeds the centrifugal force due to the cloud's spin and/or internal gas pressure. This results in a squeezing of the gas cloud together with the twisted magnetic tube. Since the top and bottom of the cloud have free boundaries for expansion along the magnetic lines of force, the cloud starts to expand in the vertical (z) direction with its volume being conserved. This expansion may occur hydrostatically with constant gas pressure and vol-

ume, unless the z directional gravity is too strong. Hence, the growth time of the tornado is on the order of the spin period, or $t \sim 2\pi r/v \sim 1.5 \text{ Myr}$, where r is the tornado radius. This is on the same order as the time scale of the propagation of a torsional Alfvén wave,

$$t_A \sim L/2V_A \sim 2.7 \text{ Myr},$$

where $L \sim 170 \text{ pc}$ and $V_A \sim 30 \text{ km s}^{-1}$. Therefore, the vertical expansion velocity of the cloud is $v_z = r_z/t \sim 14 \text{ km s}^{-1}$, if we assume the initial cloud radius in the z direction to be $r_z \sim 20 \text{ pc}$, as discussed below.

Because the vertical magnetic tube is twisted and squeezed, the spin motion of the cloud is accelerated due to angular momentum conservation. The acceleration of spin will continue until the dynamic $\beta_{\text{d:spin}}$ due to the spin reaches unity. For a spin velocity of $v \sim 30 \text{ km s}^{-1}$, as for the upper and lower parts of CO tornado, the critical magnetic strength is $B \sim 0.5 \text{ mG}$. If the spin velocity is as high as that in the high-velocity cloud G1.2+0.06, $v \sim 100 \text{ km s}^{-1}$, the magnetic field strength is required to be as strong as $B \sim 1 \text{ mG}$ for $\beta_{\text{d:spin}} \sim 1 \text{ mG}$. For both cases, the required field strengths are safely weaker than the maximum value of $B_{\text{max}} \sim 4 \text{ mG}$, corresponding to galactic rotation at $\beta_{\text{d:gal}} \sim 1$.

3.5. Acceleration of Cloud Spin

Let the initial cloud radius be r with the galacto-centric distance of the cloud center being R , and the radii of the near and far sides of the cloud being $R_1 = R - r$ and $R_2 = R + r$, respectively, with respect to the GC (figure 6), and galactic rotation velocities at R_1 and R_2 being V_1 and V_2 . The spin velocity of the cloud is therefore expressed as

$$v = (V_2 - V_1)/2.$$

We express these radii and velocities after cloud contraction toward the spin axis as R'_1, R'_2, V'_1 and V'_2 . Then, due to angular

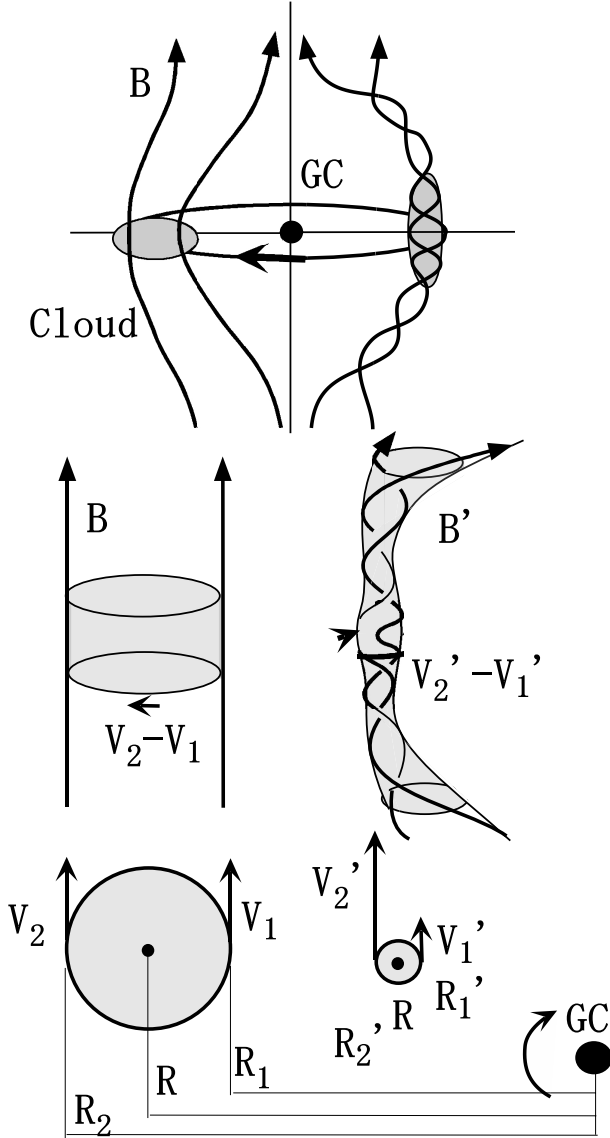


Fig. 6. Magnetic squeezing magnetic model for the GCT in the presence of a vertical ordered magnetic field.

momentum conservation, we have

$$R_1 V_1 = R'_1 V'_1 \text{ and } R_2 V_2 = R'_2 V'_2.$$

If the cloud shrinks and becomes sufficiently small, so that $r' \ll r$, we have $R'_1 \sim R'_2 \sim R$. Then, the spin velocity after contraction may be written as

$$v' = (V'_2 - V'_1)/2 \sim (R_2 V_2 - R_1 V_1)/2R.$$

If we assume that the cloud was initially rotating with the galactic disk having a flat rotation curve, we have $V_1 = V_2 = V_0$, and therefore

$$v' \sim V_0(R_2 - R_1)/2R = V_0 r/R.$$

Suppose that the CO tornado was produced from a molecular cloud of initial mass of $\sim 10^6 M_\odot$. The cloud may have been a normal-sized giant molecular cloud, and hence we may assume a cloud size of about 30 – 50 pc, or a radius of about $r \sim 20$ pc.

Alternatively, if we assume that the volume of the cloud before and after squeezing are the same, or

$$4\pi r^3/3 = \pi L r'^2,$$

where $L \sim 170$ pc is the total length of tornado and $r' \sim 7$ pc is the radius, we obtain the original radius of the cloud to be $r \sim 20$ pc. Now, let us take $R \sim 170$ pc and a galactic rotation velocity of $V_0 = 200 \text{ km s}^{-1}$. Then, after squeezing, the spin velocity is calculated to be $v \sim 25 \text{ km s}^{-1}$. This velocity is consistent with the observed spin velocity of the CO tornado.

3.6. Vertical Extent and Growth Time of Tornado

When the cloud is squeezed by the twisted magnetic field, the gas is pushed away from the galactic plane toward high latitude along the magnetic lines of force. The length L of the tornado top can be related to the initial and final size of the cloud r and r' , as above, if we neglect the gravity and assume hydrostatic expansion along the tube, while keeping the volume constant. In reality, however, the gravity toward the galactic plane would suppress the expansion, and therefore the height would be lower. Nevertheless, the estimate shows that the observed extents of the CO tornado can be easily understood by the magnetic squeezing mechanism.

We here assumed hydrostatic expansion of gas along a magnetic tube, and therefore the growth time of the tornado depends on the frequency of the cloud spin. The observed spin period is given by

$$t \sim 2\pi r'/v' \sim 1.5 \text{ Myr}.$$

This period must be compared with the galactic rotation period,

$$t_{\text{gal}} \sim R/V_0 \sim 5 \text{ Myr}.$$

We may thus consider that a squeezed magnetic tube grows on a time scale of several million years. When the cloud shrinks to a certain radius by magnetic tube squeezing, the high-velocity spin is accelerated. Then, the vertical expansion will grow on a spin time scale of a couple of million years.

3.7. Loss of Angular Momentum from a Cloud and Star Formation

According to the spin up of the cloud, the magnetic field is further twisted and the toroidal component is amplified. Not only the hydrostatical expansion, but also the gradient of the toroidal magnetic pressure in the z direction causes an upward flow of gas along the magnetic tube. This process results in a transfer of rotating gas toward high altitudes, and therefore results in the transfer of angular momentum toward the galactic halo along the twisted magnetic tube (Uchida & Shibata 1985).

This results in a loss of angular momentum of the molecular cloud in the galactic plane, and enhances the self-gravitational collapse and the formation of a dense molecular core in the central region of the cloud. This may lead to efficient star formation from the cloud, and may result in the birth of a compact stellar cluster, or possibly a globular cluster. The time scale of the angular-momentum loss will be about the same as the tornado acceleration, or several million years. This may not be sufficiently long for star formation. In fact, although we see only a very weak MSX source, no HII region is supposed to be associated with a star-forming region. Hence, the molecular cloud at the root of GCT would be on the way growing to a future active star forming region.

4. Discussion

By analyzing the CO line survey data in the Galactic Center by Oka et al. (1998), we have noticed the Galactic Center Tornado. The GCT is a collimated molecular-gas feature of 170 pc long and 14 pc wide, extending vertically from the galactic plane, and is rotating around its axis at about 30 km s^{-1} . The GCT shows a coherently extended helical structure, and is slightly waving at a wavelength of about 50 pc. The coherently extended structure may be attributed to a collimation mechanism by a large-scale ordered poloidal magnetic field. We have proposed a magnetic squeezing model of a molecular cloud in galactic rotation penetrated by a large-scale vertical magnetic field. This model seems to explain the major properties of the observed GCT.

4.1. Similar Helical Objects

The morphology of GCT is similar to that of the double-helix nebula of warm dust found by Morris et al. (2006). The GCT shows two strands of helices, which are indeed observed for the double-helix nebula. Morris et al. (2006) explain the two strands by the existence of $m = 2$ mode symmetry in the circum nuclear disk of 10 pc radius, by which the poloidal magnetic field is rapidly twisted. This idea also applies to the GCT: it is natural to consider that a molecular cloud is not round, but has significant asymmetry. The two strands of helices may be due to the $m = 2$ mode asymmetry of the driving cloud. Moreover, higher order or any kinds of asymmetries of the cloud will result in individual helical strands. This will disturb an axisymmetric cylindrical structure to exhibit multiple weaving strands of helices, as partially observed in the GCT (figures 1 to 3).

Although no direct measurement of the magnetic field has yet been obtained for these objects, we considered that it is reasonable to assume the existence of a vertical magnetic field. In fact, we have various forms of evidence for large-scale ordered magnetic fields generally running across the the galactic plane from radio continuum observations, such as the radio Arc (Yusef-Zadeh & Morris 1987; Tsuboi et al. 1986; Sofue et al. 1987) and threads (LaRosa et al. 2000; Anantharamiah et al. 1991), for which magnetic strengths of ~ 0.1 to several mG have been measured.

4.2. Alternative Magnetic Mechanisms

We called our object ‘tornado’ because of its high-velocity rotation, and an assumed quasi-hydrostatic expansion of gas in the z direction along the magnetic tube. According to the magnetic squeezing mechanism, the vertical velocity is comparable to, or smaller than, the rotational and dispersion velocities in the cloud. In this sense, the outflow along GCT is not dynamic. Moreover, the gravity toward the cloud center can be negligible in the present mechanism.

The magnetic squeezing mechanism is similar to the twisting magnetic jet and/or tower mechanisms (Uchida & Shibata 1985; Kato et al. 2004, and the literatures therein), where the gas is driven by the magneto-centrifugal force and the magnetic pressure, or to the poloidal magnetic loop model from a locally magnetized accretion disk (Kudoh et al. 2002). However, in these models, the gas disk is assumed to be gravitationally

bound to the central massive object, and is accreting to a central object in sub-Keplerian rotation. In this sense, the present squeezing model is different, where the gas is not necessarily gravitationally bound by itself or to its central object.

The magnetic mechanism proposed for GCT would generally also act to accelerate and push the gas away from the galactic disk to high latitudes. Not only the G1.2+0.0 molecular flare and GCT, but also many other off-plane extensions of molecular gas, could be explained by this mechanism. Some prominent vertical extents of molecular gas are: the Sgr B molecular complex at G0.7 + 0.1 ~ -0.3 with a vertical extent of $z \sim -50$ pc, an extremely extended CO flare at G3.2 + 0.0 ~ 0.7 with $z \sim +100$ pc and a flare at G359.2-0.1 ~ 0.5 with $z \sim +80$ pc. These might be similar structures to the GCT. However, they may be in different phases of growth and/or decay in their evolution, with GCT being in the most collimated and powerful phase.

4.3. Magnetic Tube Inflation

In order for the present mechanism be applied, the magnetic field may not necessarily be as straight and uniform as assumed above. It is possible that the GCT is a part of a larger magnetic tube having a morphology like an arch connecting to another remote root in the galactic plane, similar to a solar coronal prominence. In fact, the northern GCT is bending, and might be connected to another high-latitude structure inflating from negative longitudes, such as that seen at $l \sim -1^\circ$ at velocities $V_{\text{lsr}} \sim 40$ to 60 km s^{-1} , composing an arch above the galactic plane (see channels maps in Oka et al. 1998).

Such a large-scale arch may be produced by a Parker-type instability of a magnetic flux/tube within a galactic disk injected by a sufficient amount of cosmic rays, which is naturally expected in such an active region as the Galactic Center. Given a large-scale arch of magnetic tube, and if its lifetime is long enough compared to the galactic rotation, the magnetic squeezing mechanism will apply near to its root, in the same way as discussed for the vertical-field case.

Galactic-scale magnetic arches are indeed observed everywhere above the galactic disk of the Milky Way as numerous radio spurs (e.g., Sofue 1976), HI loops, shells, and arches (Koo et al. 1992; Hartmann & Burton 1997). The starburst galaxy NGC 253 is known to have numerous filaments and arches of dusty gas (molecular gas) with scales of several hundred pc inflating from the galactic plane (Sofue et al. 1994). These arches are interpreted as being due to magnetic flux inflation caused by Parker instability, as is well known for solar coronal prominences. The GCT could be a part of one of such galactic loop prominences magnetically inflating from the galactic plane.

4.4. Weak Magnetic Field Twist

There has been a recent debate as to whether there exists a strong magnetic field in the GC region. On one hand, evidence for localized vertical magnetic fields of mG strength has been obtained by radio continuum observations (Yusef-Zadeh et al. 1984; Morris & Yusef-Zadeh 1985; Tsuboi et al. 1986; Sofue et al. 1987; Lang et al. 1999; LaRosa et al. 2000). We have so far assumed a generally strong vertical magnetic field.

On the other hand, LaRosa et al. (2005) claim that mean

magnetic fields of scale sizes greater than ~ 50 pc would be as weak as $\sim 10 \mu\text{G}$, at most $\sim 100 \mu\text{G}$. We, here, consider if the present mechanism may also apply in a weaker mean magnetic field.

Since the magnetic squeezing mechanism utilizes the twist of a large-scale magnetic field in differential galactic rotation, the original mean field is not necessarily required to be as strong as the field required to confine the GCT (~ 0.4 mG). If a part of a uniform field, whose ends are anchored to the halo at rest, is frozen into a gas complex, such as that around G1.2+0.0, it will be twisted by the galactic rotation of the cloud complex. The twisted field will be amplified to yield a locally stronger vertical field in several rotations, until it becomes as strong as the threshold field strength, ~ 0.4 mG. Similar amplification may occur if two remote gas complexes are connected by a solar prominence-like arch of a weak magnetic tube. Differential rotation of the two clouds by rapid galactic rotation twists the arch in a similar manner to that for a uniform field case, and amplify the tube field. We thus conclude that the present mechanism applies even if the vertical magnetic field is weak.

4.5. Non-Magnetic Acceleration

We now consider the case when there is no magnetic field, or the case when the magnetic energy density is negligible compared to the kinetic energy of the interstellar gas. We may consider the following possible mechanisms due to supernova explosions, radiation pressure, and out-of-plane bombing of gas clouds from companion galaxies:

Supernovae: The estimated kinetic and gravitational energies contained in the GCT are $\sim 10^{52}$ ergs (table 1), an order of magnitude greater than the typical kinetic energy given to interstellar gas by a single type II supernova, $\sim 10^{51}$ ergs. Hence, energetically, we need at least ten supernovae for the formation of GCT. Oka et al. (2001) claim that the G1.27+0.01 hyper-energetic molecular shell has a kinetic energy of $\sim 5 \times 10^{52}$ ergs, and suggest that it may be accelerated by a series of supernova explosions.

If a similar series of supernova explosions occurred once

more in a more distant past than that responsible for the present molecular shell, and if a fraction of their kinetic energy was given to directional motion vertical to the galactic plane, the GCT could be explained energetically. However, there appears to be no evidence of a remnant of such a series of supernovae in the G1.2+0.0 region, as shown in section 2.5. Moreover, there remains a question as to how explosion-plowed interstellar gas is collimated into a narrow cylinder, like the GCT.

Radiation-pressure: As a mechanism for vertical acceleration of molecular gas, we may consider the radiation-pressure acting on dust grains included in the gas by photons from bright stellar disk and/or by active star-forming regions (Sofue et al. 1994). This mechanism works without magnetic field. However, the radiation-pressure accelerates the gas toward the opposite direction from the Galactic Center, so that the northern spur would be bent outward, e.g., toward positive longitude. This is in the opposite sense to the observed GCT's bent. Moreover, the radiation pressure would not be able to collimate the outflow in such a narrow tube as the GCT.

Galactic spray: A gas dynamical interaction of the galactic halo with the interstellar gas in companion galaxies will cause a stripping of gas from the companion, and accrete onto the central part of the main galaxy. If such stripped gas from the Magellanic Clouds (Sofue 1994) and/or from the Sagittarius dwarf companion (Ibata et al. 1994) is falling into the Galaxy, the central region would eventually experience bombing of gas clouds from the outside. Such out-of-plane infall of a cloud may result in a head-tail structure emerging from the disk, and produce sprays of gas on both sides of the galactic disk. The numerous out-of-plane molecular features in the GC region, including GCT, could be explained by such a bombing-spraying mechanism from outside. Although the spray mechanism sounds promising to explain the GCT's morphology, we need a more careful modeling and calculation to investigate if a strongly collimated structure like GCT can indeed be produced.

The author thanks Dr. T. Oka for providing him with the FITS formatted CO survey data and for the invaluable discussion and comments.

References

- Anantharamaiah, K. R., Pedlar, A., Ekers, R. D., & Goss, W. M. 1991, MNRAS, 249, 262
 Arimoto, N., Sofue, Y., & Tsujimoto, T. 1996, PASJ, 48, 275
 Handa, T., Sofue, Y., Nakai, N., Hirabayashi, H., & Inoue, M. 1987, PASJ, 39, 709
 Hartmann, D. & Burton, W. B. 1997, Atlas of Galactic Neutral Hydrogen, (Cambridge: Cambridge University Press)
 Ibata, R. A., Gilmore, G., & Irwin, M. J. 1994, Nature 370, 194
 Kato, Y., Mineshige, S., & Shibata, K. 2004, ApJ, 605, 307
 Koo, B.-C., Heiles, C., & Reach, W. T. 1992, ApJ, 390, 108
 Kudoh, T., Matsumoto, R., & Shibata, K. 2002, PASJ, 54, 267
 Lang, C. C., Morris, M., & Echevarria, L. 1999, ApJ, 526, 727
 LaRosa, T. N., Brogan, C. L., Shore, S. N., Lazio, T. J., Kassim, N. E., & Nord, M. E. 2005, ApJ, 626, L23
 LaRosa, T. N., Kassim, N. E., Lazio, T. J. W., & Hyman, S. D. 2000, AJ, 119, 207
 Morris, M., Uchida, K., & Do, T. 2006, Nature, 440, 308
 Morris, M., & Yusef-Zadeh, F. 1985, AJ, 90, 2511
 Oka, T., Hasegawa, T., Sato, F., Tsuboi, M., & Miyazaki, A. 1998, ApJS, 118, 455
 Oka, T., Hasegawa, T., Sato, F., Tsuboi, M., & Miyazaki, A. 2001, PASJ, 53, 787
 Price, S. D., Egan, M. P., Carey, S. J., Mizuno, D. R., & Kuchar, T. A. 2001, AJ, 121, 2819
 Reich, W., Fuerst, E., Reich, P., & Reif, K. 1990, A&A Supl., 85, 633
 Sofue, Y. 1976, A&A, 48, 1
 Sofue, Y. 1994, PASJ, 46, 431
 Sofue, Y. 1995, PASJ, 47, 527
 Sofue, Y. 2006, PASJ, 58, 355
 Sofue, Y., Kudoh, T., Kawamura, A., Shibata, T., & Fujimoto, M. 2004, PASJ, 56, 633
 Sofue, Y., Reich, W., Inoue, M., & Seiradakis, J. H. 1987, PASJ, 39, 95
 Sofue, Y., Wakamatsu, K., & Malin, D. F. 1994, AJ, 108, 2102

Strutskie, M. F., et al. 2006, AJ, 131, 1163

Tsuboi, M., Inoue, M., Handa, T., Tabara, H., Kato, T., Sofue, Y., &
Kaifu, N. 1986, AJ, 92, 818

Uchida, Y., & Shibata, K. 1985, PASJ, 37, 515

Yusef-Zadeh, F., Morris, M. 1987, ApJ, 322, 721

Yusef-Zadeh, F., Morris, M., & Chance, D. 1984, Nature, 310, 557.